

926
BOX 2

9

LA-9000-MS

UC-66b

Issued: November 1981

**Further Description of the Petrology
of the Topopah Spring Member of the
Paintbrush Tuff in Drill Holes UE25A-1
and USW-G1 and of the Lithic-Rich Tuff
in USW-G1, Yucca Mountain, Nevada**

P. I. Carroll*
F. A. Caporuscio
D. L. Bish

HYDROLOGY DOCUMENT NUMBER 267

*Visiting Staff Member. US Geological Survey, 1107 NW 45th Street, Seattle, WA 98105

Los Alamos Los Alamos National Lab
Los Alamos, New Mexico 87545

FURTHER DESCRIPTION OF THE PETROLOGY OF THE TOPOPAH SPRING MEMBER OF THE
PAINTBRUSH TUFF IN DRILL HOLES UE25A-1 and USW-G1 AND OF THE
LITHIC-RICH TUFF IN USW-G1, YUCCA MOUNTAIN, NEVADA

by

P. I. Carroll, F. A. Caporuscio, and D. L. Bish

ABSTRACT

The Topopah Spring Member of the Paintbrush Tuff and the Lithic-rich tuff are two Tertiary volcanic units that occur in cores from drill holes UE25a-1 and USW-G1 at Yucca Mountain, Nevada. Recently they have been suggested as possibly suitable for the permanent storage of high-level radioactive waste. This report augments earlier petrologic characterization of these units.

The Topopah Spring Member (approximately 350 m thick) has two compound cooling units. The upper, thinner unit is densely welded to vitrophyric. The lower unit ranges from nonwelded to vitrophyric, and its nonwelded base is extensively zeolitized to clinoptilolite and mordenite. Heulandite occurs as fracture fill in the overlying vitrophyric part, but zeolites are absent above that vitrophyre. Here primary devitrification plus vapor-phase crystallization dominate the mineralogy. Vapor-phase effects are especially prominent between the two vitrophyres in both cores and include numerous large lithophysal cavities throughout most of this moderately to densely welded tuff.

The Lithic-rich tuff extends from 1203 to 1506 m in the USW-G1 drill core. It is nonwelded to partly welded but is well indurated due to pervasive intergrowths of authigenic minerals. These phases are analcime, albite, alkali feldspar, sericite, chlorite and quartz. The transition from analcime to secondary albite corresponds to Iijima's zeolite Zone IV boundary, and this boundary appears in USW-G1 at 1326 m. However, analcime remains as a prominent phase through most of the Lithic-rich tuff.

Further work is necessary to assess the suitability of either of these horizons for a waste repository. In the Topopah Spring Member, both mechanical and hydrologic properties of the thick lithophysal zone must be studied, as well as the complete sequence of fracture fill. For both units, zeolite and clay mineral stabilities need to be investigated.

I. INTRODUCTION

A. Background of Waste-Storage Effort

The possibility of permanent storage of high-level radioactive waste in deep, mined repositories has been and is currently being studied for various rock types in the United States. A major effort of this project is the investigation of tuff at the Nevada Test Site (NTS) as a suitable repository medium. A comprehensive exploration program of the thick sequence of tuff underlying Yucca Mountain (located near the southwestern boundary of the NTS) was begun in 1979. Cored holes have been drilled to investigate the stratigraphy, structure, and petrology of the Yucca Mountain area as a part of this program. Los Alamos National Laboratory shares responsibility with the US Geological Survey for characterization of the stratigraphy and petrology of these cores and is especially responsible for identification and description of the core minerals on a microscopic scale.

B. Purpose of this Report

This report is concerned with core samples from two exploration drill holes that were previously studied at Los Alamos: drill holes UE25a-1 (Sykes et al. 1979) and USW-G1 (Bish et al. 1981). The latter report will hereafter be referred to as the G1 report. In that report, four units in the USW-G1 core were suggested to have favorable characteristics for a waste repository. The units, listed in order of increasing depth in the drill hole, are: the lower cooling unit of the Topopah Spring Member of the Paintbrush Tuff; the lower cooling unit of the Bullfrog Member of the Crater Flat Tuff; the Tram tuff (informal; Spengler et al., in preparation); and the Lithic-rich tuff (informal; Spengler et al., in preparation). The latter three units were not cored in hole UE25a-1.

Prior to the completion of the G1 report, the Topopah Spring and the Lithic-rich tuff had not been given major consideration as repository horizons, and upon completion of the report, it was thought necessary to provide a description of these units in USW-G1 and UE25a-1, which would be comparable in detail to that of the Bullfrog and the Tram tuff in the G1 report. Specifically, the presentation of the Topopah Spring in the UE25a-1 report (Sykes et al. 1979) did not include any detailed x-ray analysis of the clay minerals, iron-titanium oxide average oxidation states were not examined, and alteration/devitrification processes were not interpreted in detail.

Furthermore, the G1 report described core samples from only the lowermost portion of the lower cooling unit of the Topopah Spring Member.

The purpose of this report is to provide a reasonably complete petrologic-stratigraphic description of these two units in USW-G1 and UE25a-1. To achieve this goal, some information contained in the previous reports is included in this report, but no attempt is made to thoroughly discuss or supplant those descriptions.

C. Methods and Types of Observations

Three instruments were utilized extensively in the petrologic descriptions reported here. A Siemens model D-500 x-ray diffractometer was used for mineral identification in powdered bulk samples and to analyze the clays in a few samples. A polarizing petrographic microscope (reflected and transmitted light) was used to examine thin sections, enabling description of such features as degree of welding, effects and products of primary devitrification, vapor-phase alteration, secondary alteration, zeolitization, clay alteration, and opaque mineral average oxidation state, as well as the kinds and abundance of original constituents (shards, pumice fragments, phenocrysts, groundmass, and lithic fragments). Lastly, a Cameca (Camebax) automated electron microprobe assisted or confirmed the identification of phenocrysts and authigenic phases.

II. FOREWORD: COMMENTS ON PETROLOGIC OBSERVATIONS

Explanation of a few of the petrologic observations that are frequently made in this report can best be given here instead of within the presentation of results. Degree of welding is a common and important description of an ash-flow tuff but has only subjective meaning if the terms are not defined. Our working classification of degree of welding is given below (Table I). It is subjective but should give a better image of the rock we are describing.

At least four processes can profoundly alter the appearance of a tuff in thin section. These are: (1) primary devitrification (alteration of glass to crystalline materials during cooling of the ash-flow sheet); (2) vapor-phase crystallization (growth of crystals promoted or initiated by the presence of a vapor phase pervading the ash-flow sheet during cooling); (3) authigenic recrystallization (here used to denote further recrystallization of crystalline material after cooling and restricted mainly to growth of new silica minerals and alkali feldspars); (4) secondary mineral growth after cooling --

TABLE I

EXPLANATION OF TERMINOLOGY CONCERNING DEGREE OF WELDING IN THIN SECTION

Nonwelded	-- No deformation of components.
Slightly welded	-- Minor shard deformation around phenocrysts.
Partly welded	-- Major shard deformation around phenocrysts; no flow deformation in groundmass.
Moderately welded	-- Major shard deformation around phenocrysts; deformation and flow in groundmass.
Densely welded	-- Pronounced shard deformation and alignment.
Vitrophyric	-- Glassy, all vitric components annealed (perlitic fractures may occur).

chiefly the replacement of glass and other phases by zeolites, clay minerals, opal, etc. Description of the effects of these processes in thin section constitutes a large part of this report.

Following the work of Haggerty (1976), it is possible to recognize exsolution phases in opaque minerals and use them to arrive at empirically determined oxidation states for the opaque minerals. Oxidation states can be determined for both cubic (C_1 - C_7) and rhombohedral (R_1 - R_7) exsolution phases, where increasing subscripts indicate increasing oxidation state (1 = not oxidized, 7 = completely oxidized). Because oxidation states typically are similar for both the rhombohedral and cubic phases, we use only the C_x labels for simplicity. Generally, the oxidation state of the opaque oxides correlates inversely with the degree of welding. The average oxidation states recorded need not necessarily, and most probably do not, record the current oxidation state of the rock in situ.

III. RESULTS

A. Topopah Spring Member of Paintbrush Tuff

1. USW-G1 Core. The Topopah Spring Member in the USW-G1 core extends from a depth of 71.6 to 434.3 m. The G1 report thoroughly describes the core from 363 to 434.3 m (near the basal vitrophyre), but above that interval, only x-ray analysis had been performed for earlier reports. Thus, to complete the

coverage, descriptions of thin sections from six samples above 363 m are added in this report. Table II summarizes the stratigraphy of the Topopah Spring in the USW-G1 core and lists the depths of samples from which thin sections were made.

TABLE II
STRATIGRAPHY AND SAMPLING OF THE TOPOPAH SPRING MEMBER IN THE USW-G1 CORE

<u>Lithologic Groups^a in the USW-G1 Topopah Spring Member</u>	<u>Top and Bottom of Interval in Core (depths in m)</u>	<u>Depths in Core (m) of Samples Thin-sectioned and Described Either in This or the USW-G1 Report</u>
Nonwelded ash-flow tuff	71.6-82.3	--
Vitrophyre	82.3-85.3	--
Densely welded ash- flow tuff (quartz- latitic caprock)	85.3-89.0	89.0
Densely welded ash- flow tuff	89.0-139.0	137.2
Ash bed	139.0-139.3	--
Densely welded ash- tuff	139.3-392.3	153.6, 188.9, 220.1, 230.7 Samples above dashed line are new in this report.

		Samples below are from USW-G1 report. 363, 378, 392
Vitrophyre	392.3-409.0	394
Moderately welded to nonwelded ash-flow tuff	409.0-427.9	424
Bedded reworked tuff	427.9-434.3	--

^a Summarized from the detailed stratigraphy of the US Geological Survey core log of USW-G1 (Spengler et al., in preparation).

The two thin-section samples above the ash bed at 139 m are moderately (137.2 m) and moderately to densely (89 m) welded and devitrified. Devitrification is evidenced by axiolitic texture in shards and by fibrous aggregates of silica and alkali feldspar occurring as small spherulites throughout pumice fragments and as linings (parallel or radiating) inside pumice borders. Vapor-phase crystallization is observed in the growth of tridymite (only optically identified in the higher sample) in void spaces in shards, pumice fragments, and groundmass. Further evidence of vapor-phase crystallization in the sample at 137.2 m consists of large spherulites in pumice fragments and relatively coarse-grained quartz and alkali feldspar crystals in the centers of shards. The groundmass of both samples contains clay, but in the sample at 89 m, the groundmass is nearly isotropic, suggesting that much is still glass. At 137.2 m, minute crystals (probably quartz and feldspar) are abundant in the groundmass.

Phenocrysts are abundant in both samples, although more so in the upper sample than the lower. The phenocrysts common to these two samples are quartz, plagioclase and alkali feldspars, biotite, magnetite, and minor allanite. The biotite is blackened by opaque acicular crystals parallel and occasionally perpendicular to cleavage. The upper sample also has clinopyroxene, and a calcite vein occurs in the sample at 89 m. Lithic fragments are present in both samples.

Below the ash bed there is a section of ash-flow tuff described by Spengler et al. as densely welded, beneath which is the vitrophyre described in the G1 report. These rocks and the underlying moderately welded to (grading downward) nonwelded ash-flow tuff probably represent a single cooling unit. Description of these rocks will be in two parts, the first covering the samples not reported in the G1 report, all of which are above the vitrophyre, and the second reviewing the samples described in that report.

Below the ash bed, the thin-section samples not described in the G1 report are densely welded or (at 153.6 and 230.7 m) moderately to densely welded, devitrified, and show the effects of vapor-phase crystallization. Pumice fragments frequently show a border region of spherulitic or parallel aggregates of fibrous silica and feldspar indicative of primary devitrification but are dominated by vapor-phase crystallization. The latter process produces large, occasionally zoned spherulites, and relatively coarse grained quartz, alkali feldspar and tridymite in central regions of relict pumice clasts.

A minor proportion of the shards in all samples show axiolitic texture, but the more common primary devitrification texture consists of replacement of shards by fibrous radial aggregates of silica and alkali feldspar, either crossing or confined within shard boundaries. Vapor-phase effects in shards are noticeable only in the samples at 153.6 and 230.7 m, and consist of granophyric texture in both samples and tridymite in the deeper sample.

In the groundmass of all the samples in this section, secondary clays and numerous roughly circular pockets filled with tridymite (vapor phase) are found. However, the bulk of the groundmass consists of silica and alkali feldspar, either as a very fine grained crystalline aggregate or as fibrous, brown, radial aggregates. The latter texture is the one described in the preceding paragraph as overprinting shards and in both cases is interpreted as a result of primary devitrification. The texture is first seen in the groundmass at 153.6 m and becomes progressively more pervasive in both shards and groundmass in the next three samples (188.7, 220.1, and 230.7 m). In the last sample, the texture obliterates primary textures over large portions of the thin section.

The phenocrysts in these samples are not abundant and generally consist of plagioclase and alkali feldspars, magnetite, quartz (minor to absent), and minor blackened biotite.

In each of the samples not described in the G1 report (above and below the ash bed), three plagioclase and three potassium-feldspar phenocrysts were analyzed using the microprobe. The only exception to this was one very crystal poor sample (at 220.1 m), for which only two crystals of each feldspar were analyzed. The results are summarized in Table III. The typical compositions are sanidine and oligoclase. In comparing this suite of samples, a strong homogeneity is evident in the compositions of each of the two feldspar phenocryst types, and these average compositions compare well with the phenocrysts lower in the Topopah Spring as reported in the G1 report (see Bish et al. 1981).

Above the vitrophyre, the three densely welded samples described in the G1 report are similar to the samples just discussed. All are densely welded, devitrified, and have undergone vapor-phase crystallization. The devitrification spherulites and sprays that had become so prominent in the sample at 230.7 m are, at 363 and 378 m, smaller and more restricted to bands of flattened shards. The spherulites do cross vitric boundaries but tend to preserve

TABLE III

ANALYSES BY MICROPROBE OF FELDSPAR PHENOCRYST COMPOSITIONS FOR TOPOPAH SPRING MEMBER SAMPLES
NOT DESCRIBED IN THE USW-G1 REPORT

Sample Depth (in m)	Potassium Feldspar			Plagioclase Feldspar		
	% NaAlSi ₃ O ₈ (Ab)	% KAlSi ₃ O ₈ (Or)	% CaAl ₂ Si ₂ O ₈ (An)	% NaAlSi ₃ O ₈ (Ab)	% KAlSi ₃ O ₈ (Or)	% CaAl ₂ Si ₂ O ₈ (An)
89	48	48	4	76	7	17
	46	50	4	65	9	26
	49	48	3	70	7	23
137	52	45	3	74	7	19
	47	50	3	74	9	17
	48	49	3	74	12	14
154	56	40	4	78	6	16
	51	46	3	76	7	17
	50	47	3	77	7	16
189	41	58	1	64	3	33
	47	51	2	77	6	17
	42	57	1	78	6	16
220	41	58	1	77	8	15
	46	52	2	77	6	17
231	46	53	1	79	6	15
	51	47	2	79	6	15
	46	53	1	78	5	17

primary textures, in contrast to the sample at 230.7 m. The samples at 363 and 378 m also have a stronger eutaxitic foliation composed of layers of flattened shards (now fibrous aggregates) and of pumices (now finely crystalline lenses).

Vapor-phase effects, such as the presence of lithophysae and large bordering spherulites in pumice fragments, are still observed in these three samples, but post-cooling authigenic recrystallization has begun to alter the rock. The groundmass and interiors of pumice fragments in places are recrystallized to coarser patches of quartz and alkali feldspar and, in the sample at 363 m, some of the circular vugs originally filled with tridymite have recrystallized to polycrystalline quartz. Below 363 m, no sample of the Topopah Spring shows these vugs.

The sample at 392 m, 0.3 m above the vitrophyre, is distinctive in that it is less compacted than the next higher sample and the shards are devitrified to a distinctive fibrous radial aggregate, reddish-brown in plane light and showing an anomalous bluish extinction under crossed polars. A very similar rock (sample YM-30) was described by Sykes et al. (1979) just above the basal vitrophyre of the Topopah Spring in the UE25a-1 core. They labeled this aggregate as montmorillonite, but it is more likely that it is an intergrowth of silica and alkali feldspar, with disseminated clays, rutile, and hematite.

The vitrophyre, strongly compacted and densely welded, is composed largely of unaltered glass showing abundant perlitic fractures. The sample below (at 424.3 m) is slightly to partly welded and most is unaltered glass, although minor clinoptilolite fills voids in shards and pumice fragments.

The phenocrysts are very similar to those in the samples already discussed -- very minor in abundance and composed of two feldspars (compositions are sanidine and oligoclase), opaque minerals, and rare quartz and biotite. Altered pyroxene phenocrysts are in trace amounts at 424.3 and 378 m.

2. UE25a-1 Core. The Topopah Spring Member was cored in the UE25a-1 drill hole and is described in Sykes et al. (1979).

As an introduction to the thin-section descriptions, the results of x-ray diffraction analyses of samples from the UE25a-1 core made for this report (Table IV) will be presented first. X-ray analyses are of the same samples of core (22 in number) from which the thin sections described by Sykes et al. (1979) were made. These thin sections are further described later in this report. Powder samples were obtained by grinding homogeneous samples of core approximately 1 cm^3 in size and were placed in cavity mounts for x-ray

TABLE IV

APPROXIMATE MINERAL ABUNDANCES (% OF SAMPLE) IN TOPOPAH SPRING MEMBER SAMPLES FROM UE25A-1 DRILL CORE,
BY X-RAY DIFFRACTION ANALYSIS

Sample Number	Depth (m)	Depth (ft)	Smectite	Mica	Clino- ptilolite	Morden- ite	Analcime	Quartz	Cristo- balite	Alkali Feldspar	Calcite	Glass	Tridymite
YM-6	84	277	~5	5-15	-	-	-	-	-	15-30	-	55-80	-
YM-7	102	335	<5	5-15	-	-	-	-	5-20	50-70	-	-	5-15
YM-8	137	450	5-15	-	-	-	-	5-10	5-20	40-60	-	-	-
YM-9	143	469	5-15	-	-	-	-	5-10	5-20	40-60	-	-	-
YM-9	Clay Fraction 10±10% illite randomly interstratified with montmorillonite												
YM-20	206	667	5-10	-	-	-	-	40-50	5-15	40-50	-	-	-
YM-20	Clay Fraction 35 ±10% illite randomly interstratified with montmorillonite												
YM-21	223	733	5-10	<5	-	-	-	40-50	5-15	40-50	-	-	-
YM-17	227	744	5-10	<5	-	-	-	30-40	5-20	40-60	-	-	-
YM-18	255	836	5-10	-	-	-	-	40-60	-	40-60	-	-	-
YM-22	258	848	5-10	-	-	-	-	40-60	-	40-60	-	-	-
YM-19	268	879	5-15	<5	-	-	-	40-60	-	40-60	-	-	-
YM-23	272	894	5-10	-	-	-	-	40-60	-	40-60	-	-	-
YM-24	286	937	<5	-	-	-	-	40-60	-	40-60	-	-	-
YM-25	308	1012	<5	~5	-	-	-	40-60	-	40-60	-	-	-
YM-26	323	1061	<5	-	<10	-	-	50-60	-	30-50	-	-	-
YM-27	339	1112	5-15	5-10	-	-	-	40-60	-	40-60	-	-	-
YM-28	351	1153	5-15	-	-	-	-	40-60	-	35-55	-	-	-
YM-29	364	1195	5-10	-	-	-	-	40-60	-	40-60	-	-	-
YM-30	385	1264	5-10	~5	5-10	-	-	40-60	5-15	30-50	-	-	-
YM-31	390	1279	10-20	-	<10	-	-	<10	10-20	5-15	-	50-80	-
YM-31	Clay Fraction 20±10% illite randomly interstratified with montmorillonite												
YM-32	403	1324	5-15	-	60-80	~5	-	5-10	-	5-10	-	-	-
YM-32	Clay Fraction 25±10% illite randomly interstratified with montmorillonite												
YM-34	414	1358	~5	-	60-80	5-10	-	5-15	-	5-10	-	-	-
YM-35	421	1382	~5	-	50-70	30-50	-	-	-	-	-	-	-

diffraction. In addition, the clay fraction was separated from four powder samples via sedimentation and centrifugation, and the clays were examined using oriented mounts under a variety of conditions (air dry, 110°C, and ethylene-glycol solvated). The results are semiquantitative only, and percentages for cristobalite are unreliable due to complete overlap with the alkali feldspar patterns. Minimum detection limits for most phases range between 1 and 5%. The type of smectite present was determined using cavity sample mounts, and the degree of interstratification with illite was determined by comparing the observed x-ray patterns of ethylene-glycol solvated smectite with patterns calculated by the method of Reynolds et al. (1970).

Noteworthy aspects of the results are as follows:

- (1) There is an upper (84 m) and a lower (389 m) vitrophyre.
- (2) Quartz first appears at 137 m and increases in abundance through 385 m.
- (3) Tridymite occurs at 102 m.
- (4) Clinoptilolite first appears at 323 m and is a dominant phase below 395 m.
- (5) Mordenite first appears at 403 m and increases downward.
- (6) Smectites are present in most samples but are virtually absent above 90 m and between 286 m and 323 m.
- (7) Micas, probably biotite, are sporadically distributed and are never dominant components of the tuff. One of the samples (YM-27) yields a broad 10 Å peak suggesting the presence of either illite or an oxidized/altered biotite.
- (8) The clay fractions examined contain montmorillonite randomly interstratified with illite. The clay at 143 m is almost pure montmorillonite with $10 \pm 10\%$ illite interstratified. The montmorillonite at 206 m has substantially more interstratified illite, $35 \pm 10\%$. The montmorillonites at 390 m and 403 m are similar, having $20 \pm 10\%$ and $25 \pm 10\%$ interstratified illite, respectively. The degree of interstratification is important because the cation exchange capacity and water loss on heating both decrease with an increase in interstratified illite. The basal spacings of the ethylene-glycol complexes suggest that the layer charges increase with depth. The spacings of the air-dry montmorillonites at 143, 206, and 390 m suggest that these clays are magnesium and sodium saturated, and the

montmorillonite at 403 m appears to be sodium saturated. Future work will be done in an environmental cell on the x-ray diffractometer to examine the hydration states of the smectites as a function of temperature and humidity.

The Topopah Spring Member is approximately 331 m thick in the UE25a-1 drill hole, and the sections indicate at least six discrete portions of two compound ash-flow cooling units. The basal portion (403 to 421 m) is nonwelded and heavily zeolitized. Immediately overlying is a basal vitrophyre (385 to 390 m), which is in part devitrified. Above the basal vitrophyre is a thick sequence (255 to 364 m) of devitrified, densely welded ash-flow tuff that has both vapor-phase crystallization and granophyric textures. From 206 to 227 m is a zone of moderately welded, devitrified ash-flow tuff with moderate vapor-phase crystallization. Finally, at the top of the sequence is a densely welded zone (84 to 137 m) with extensive vapor-phase crystallization that correlates to the quartz-latitude caprock of Lipman et al. (1966), overlain by a second vitrophyre.

The nonwelded basal section of the Topopah Spring (samples YM-32 to -35) is heavily zeolitized. Clinoptilolite is the predominant zeolite phase in sample YM-32, with only minor mordenite. However, in the progression downward through the nonwelded ash flow, mordenite increases in abundance until it is subequal to clinoptilolite. Another mineralogical change with depth is the distribution of the clays in the samples. In YM-32, most clays are concentrated along shard boundaries and pumice tube walls, with only minor clays elsewhere in the groundmass. The clay content in the groundmass increases steadily with depth. The clay content also increases along pumice tube walls until clays are the dominant textural feature in pumice lapilli of YM-35.

Texturally, these samples resemble the zeolitized portion of the nonwelded flow in the G1 hole. Shards are typically large, undeformed and are completely pseudomorphed by zeolites and clays. Shard borders are rimmed by rutile and clays, which are perpendicular to the boundaries. Inner voids also commonly have terminated clinoptilolite and minor acicular mordenite partially infilling the region. Pumices are pseudomorphed by clinoptilolite, with smectite clays lining tube walls. Groundmass phases in the nonwelded ash flow are fine-grained clinoptilolite, oxides, and clays. As mentioned in the previous paragraph, mordenite becomes more prominent and manifests itself as very small spherulites or acicular sprays. Phenocrysts include quartz, plagioclase, and

alkali feldspar. Lithic fragments are mostly welded tuff and minor lava clasts.

The basal vitrophyre of the Topopah Spring Member is represented by samples YM-30 and -31 (385 and 390 m, respectively). Sample YM-30 shows primary devitrification in the form of large, sprawling spherulites which crosscut all vitric boundaries. Shards have dark brown cores due to clay concentrations whereas pumice lapilli and shard rims are tan (low clay concentration). Some portions of the pumice are composed of very fine grained granular quartz and alkali feldspar in random patches. Veins in YM-30 are filled with heulandite (Sykes et al. 1979) and montmorillonite. YM-31 is still predominantly glass with rutile and smectite clays aligned parallel to pumice tube walls. Perlitic cracks are abundant in the sample and transgress all boundaries. Veins in this sample are filled by heulandite and/or montmorillonite and rutile. Phenocrysts in both samples of the basal vitrophyre are plagioclase, alkali feldspar, quartz, biotite, and iron-titanium oxides.

Above the vitrophyre is a thick sequence of densely welded, devitrified ash-flow tuffs. The sample numbers are YM-18, -19, -22 to -29, and sample depths range from 255 to 364 m. All samples show primary devitrification, vapor-phase crystallization, and granophyric textures resulting in alkali feldspar and silica phases. For the most part, primary devitrification textures are relict or have been overprinted by later authigenic processes. Ubiquitous phenocrysts in this densely welded zone are plagioclase, quartz, and alkali feldspar. Commonly, biotite, magnetite, and hornblende also occur.

Shard morphologies are fairly consistent throughout this densely welded portion of the Topopah Spring Member. Typically the outer border region is composed of fibrous quartz and alkali feldspar intergrowths oriented perpendicular to shard borders. These intergrowths also crosscut shard boundaries and slightly encroach into the groundmass. Growing inward from the fibrous zone, and in some places in optical continuity with the sprays, are terminated vapor-phase crystals (quartz and alkali feldspar) that partially fill the central regions of the shards. In the center of the shards are granophyric patches of large, interlocking quartz and alkali feldspar grains. This sequence is by far the dominant shard morphology in the densely welded tuffs from YM-18 to YM-29. Three other shard morphologies also are present but only in small amounts in samples YM-25 to YM-29. They are (1) axiolitic shards, (2) shards totally dominated by vapor-phase terminal and granular grains of

quartz and alkali feldspar, and (3) shards composed of fibrous sprays (quartz and alkali feldspar) that lie parallel to outer boundaries. Shards of samples YM-18, -19, -22 to -24, and -28 all have a predominance of vapor phase and granophyric crystallization textures. In samples YM-25 to -27 the vapor-phase and granophyric textures share equal status with types (1) and (2) above. Sample YM-29 has type (3) morphology in addition to the general case.

Pumice morphologies in the thick, densely welded portion all possess common characteristics. First, the border regions are indistinct and composed of granular to fibrous quartz and alkali feldspar intergrowths that cross boundaries and intrude on the groundmass. Next, large spherulites and lithophysae showing numerous growth stages fill most of the central lapilli regions. These spherulites cross and obliterate most original textures. Vapor-phase crystals (quartz and alkali feldspar) partially fill the rest of each pumice fragment, with remaining interstitial areas filled by products of granophyric crystallization. Samples YM-19, -24, -28, and -29 have the largest regions of granophyric crystallization in their pumice lapilli. Less than average amounts of granophyric central regions are evident in samples YM-22, -23, and -27. An additional feature is small pockets of tridymite lined by chalcedony randomly scattered through pumice lapilli. This feature is seen in samples YM-25 to -29. In rare instances, original pumice-tube structures and accompanying small primary devitrification spherulites can be observed.

Groundmass textures can be broken into two distinct groups, the first consisting of dark brown clay-rich regions of spherulitic, fibrous or sheaf-like intergrowths of quartz and alkali feldspar with minor oxides. This is the dominant texture in samples YM-18, -19, -23, and -24. The other groundmass texture is composed of equant, fine- to medium-grained interlocking quartz and alkali feldspar grains. These areas are light tan and clay-poor. This feature predominates in YM-22 but all other samples have varying amounts of the two groundmass textures.

Other features worth mentioning in the densely welded ash-flow zone from 255 to 364 m are vein fill and lithophysal cavities. Samples YM-22 and -19 have obvious quartz veins with associated alteration of the wall rock, including all fibrous phases, to a microcrystalline granular aggregate. Samples YM-23, -25, and -26 all have one or more large lithophysal cavities.

Above the thick, densely welded portion of the Topopah Spring is a moderately welded devitrified ash flow at least 51 m thick. The three samples

observed in thin section are YM-20, -21, and -17. All three are devitrified and show extensive vapor-phase crystallization and alteration and incipient granophyric crystallization. Shards of YM-17 and -21 are dark brown due to high clay concentrations and have fibrous sheafs of radiating quartz and alkali feldspar oriented parallel to the long dimension of the shards. These sheafs do not cross vitric boundaries. Sample YM-20 also contains this shard morphology in addition to axiolitic shards and shards replaced by granular quartz and alkali feldspar.

Pumice lapilli in the moderately welded portion all have very indistinct borders and an outer region composed of fibrous or granular quartz and alkali feldspar. Small spherulites are also common in the border region. Large sprawling spherulites are common in the central portions of the lapilli with vapor-phase mineralization partially filling interstitial regions. The vapor-phase minerals are quartz and alkali feldspar only in the lowest sample (YM-17). Minor tridymite is present in YM-21 (the next higher sample) in interstitial pumice regions affected by vapor-phase crystallization. The highest moderately welded sample (YM-20) has abundant tridymite along with vapor-phase quartz and alkali feldspar in interstitial pumice regions. In addition, most of these vugs are lined with chalcedony.

Many vitric textures are completely obliterated or masked by vapor-phase crystallization and alteration. In all cases the groundmass is very fine grained, granular in appearance, and composed of quartz, alkali feldspar, clays, and oxides. In some regions the groundmass is much larger in grain size and may represent incipient granophyric crystallization. Often, in the vicinity of tridymite-filled pockets, all vitric components are changed to the above-mentioned granular texture. Plagioclase is the most common phenocryst in the moderately welded portion of the Topopah Spring Member. Lesser amounts of alkali feldspar, quartz, biotite, and iron-titanium oxides also occur as phenocrysts.

The upper densely welded zone (YM-7 to -9) immediately above the moderate welding zone corresponds to the quartz latite caprock of Lipman et al. (1966). This portion of the Topopah Spring exhibits extreme vapor-phase crystallization and alteration. The effect is so profound that most vitric textures have been masked in the samples. Vapor-phase crystallization manifests itself as large spherulites showing multiple growth stages that transgress vitric boundaries, pockets of tridymite lined by chalcedony, fine-grained patchy granular

intergrowths of quartz and alkali feldspar, and granophyric crystallization. When shards are observed in the three samples, they have unusual textures. In YM-9 (143 m), three dominant shard morphologies are present. In much of this sample, spherulites overprint the groundmass, shards, and pumice. Second, some of the recognizable shards have granophyric textures of quartz and alkali feldspar with tridymite crystals in the core regions. Third, other shards are replaced by fibrous cristobalite and alkali feldspar sheafs oriented parallel to the long dimension of the shards. No shards are discernible in YM-8, and the only shards observed in YM-7 are comparable to the second textural case stated above.

Pumice lapilli in the upper welded zone have the same features in all three samples. In every case the borders are very indistinct and have been transgressed by large spherulites. The spherulites fill and extend beyond most of the pumice clasts. They are composed of cristobalite and alkali feldspar intergrowths and typically have a mottled appearance. This mottling may be due to the presence of long stringers of clays and oxides oriented parallel to the spherulite fibers. The groundmass of all samples is composed of spherulites or patches of granular cristobalite and feldspar intergrowths. Finally, in all three samples there are abundant ovoid pockets of tridymite crystals. Many pockets are lined by a thin zone of chalcedony. The tridymite ovoids are dispersed throughout the samples but are concentrated particularly in the pumice lapilli.

All three samples have fairly abundant clays. Phenocrysts of this densely welded zone are predominantly alkali feldspar, with minor plagioclase, magnetite and biotite. No quartz phenocrysts were observed.

The highest sample observed (YM-6) in the Topopah Spring Member of the UE25a-1 drill core is a vitrophyre. It is approximately 18 m above sample YM-7 and may indicate the most densely welded zone of the quartz latite cap-rock. Vitric components of this sample are glass but are rimmed by clays and oxides. In fact, rutile and hematite, which are disseminated throughout the sample, impart a bright red color to the glass. Phenocrysts are alkali feldspar, plagioclase, biotite, magnetite, spinel(?), and clinopyroxene in YM-6. Orthopyroxene was reported by Sykes et al. (1979) in this sample, but only one possible orthopyroxene crystal was observed in thin section, rimmed by clinopyroxene.

In effect, the Topopah Spring Member of the UE25a-1 drill core is composed of two discrete compound cooling units. The lower cooling unit includes all samples from YM-17 to YM-35 and extends from at least 206 to 422 m. It is complex and comprises (in ascending order) a nonwelded zeolitized interval overlain by a thick vitrophyre, followed by a thick devitrified densely welded interval, and topped by a moderately welded devitrified interval. Separating this unit from the overlying compound cooling unit is a thin airfall bed (Spengler et al. 1979).

The upper cooling unit consists of samples YM-6 to YM-9 and includes a densely welded devitrified interval and an overlying vitrophyre. At least 59 m of ash flow make up this cooling unit, which extends from 84 to 143 m in the drill core.

Possibly, the lower cooling unit was erupted, and while it was still hot and undergoing vapor-phase activity, the upper cooling unit was emplaced. The upper ash flow was erupted at an extremely high temperature and had the effect of moderately welding the top of the lower unit and the airfall. In essence, the thermal blanketing of the upper unit never allowed the lower unit to have a nonwelded top. Vapor-phase activity was continuing in the lower unit while the hot upper vitrophyre was consolidating. This unusual timing sequence is supported by the following observations.

Vapor-phase crystallization is not present in sample YM-29, which is just above the lower vitrophyre (from which the vapor phase was emanating). Lack of vapor-phase minerals is a common phenomenon directly above a vitrophyre. The densely welded zone in the lower cooling unit shows prominent vapor-phase crystallization, but, in the moderately welded zone above, vapor-phase alteration begins to wane. Above the airfall unit, however, the densely welded portion of the upper cooling unit shows vapor-phase crystallization so prevalent as to nearly obliterate all original textures. Perhaps the overlying upper vitrophyre acted as a blanket to block and concentrate the remaining vapor phase.

3. Oxidation States of Opaque Oxides in USW-G1 Topopah Spring Samples Not Described in the USW-G1 Report, and in UE25a-1 Samples of the Topopah Spring Member. The empirical oxidation states of iron-titanium oxides in the USW-G1 and UE25a-1 cores of the Topopah Spring were determined by the use of oxidation exsolution textures (Haggerty 1976). The exsolution phases and textures were determined by reflected-light microscopy and oil-immersion lens

techniques. As stated previously, generally iron-titanium oxide oxidation states are high (C_6 - C_7) in nonwelded tuff and low (C_1 - C_2) in densely welded tuff. For example, in the UE25a-1 core, sample YM-35, a nonwelded tuff, has an average oxidation state of C_6 . Conversely, the opaque minerals of YM-20 (densely welded) show an oxidation state of C_1 .

Two other processes can have a pronounced effect on the oxidation state of the iron-titanium oxides. The first process is vapor-phase crystallization during cooling of the ash flow. Because the vapor phase is often water-rich, it can greatly increase the oxidation state of the opaque minerals. Oxides in the densely welded samples of the Topopah Spring often exhibit an average oxidation state higher than would be expected for the degree of welding. The same samples, however, are permeated with vapor-phase crystallization. Close to a vapor-phase pocket, the oxides show maximum oxidation, whereas an appreciable distance away, they are relatively unaltered (C_2 - C_3). Thus, proximity to sites of vapor-phase activity can reverse the typical inverse relationship of oxidation state to degree of welding.

The second process is the movement of ground water through fractures in otherwise impermeable tuff. The process can oxidize opaque oxides in densely welded tuff. As an example, YM-31 is a vitrophyre and should be unoxidized but shows maximum oxidation (C_7). Water flowing through the abundant perlitic fractures in the vitrophyre could have oxidized the iron-titanium oxides.

The oxidation states determined for UE25a-1 and USW-G1 samples of the Topopah Spring are given in Table V.

4. Topopah Spring Summary. The Topopah Spring Member of the Paintbrush Tuff possesses very similar petrographic characteristics in both the UE25a-1 and USW-G1 cores. Both sections are thick, with a total of 363 m in G1 and >331 m in UE25a-1. The Topopah Spring cores from both drill sites are composed of two major cooling units. The upper cooling unit of each consists of a densely welded horizon (quartz-lathite caprock) overlain by a vitrophyre. The G1 core has a nonwelded ash flow above this vitrophyre, which was not sampled (Spengler et al., in preparation). Because of an 8-m gap in UE25a-1 samples, the possibility exists that this core also has a nonwelded ash-flow top in its upper cooling unit.

The lower cooling unit in both drill cores contains nonwelded ash-flow tuff, which forms the base. This tuff grades upward into a vitrophyre that is characteristic of both cores. Overlying the vitrophyre in each core is a

TABLE V

OXIDATION STATES OF FE-TI OXIDES IN THE UE25A-1 AND USW-G1 CORES OF THE TOPOPAH SPRING MEMBER

Sample Number, Depth (in m)	Rock Description	Oxidation States	
		Average	Range
YM-6, 84	Densely welded ash-flow tuff	C ₄	C ₂ -C ₆
YM-9, 143	Densely welded, with vapor phase	C ₃	C ₂ -C ₇
YM-20, 206	Moderately welded, with vapor phase	C ₁	C ₁ -C ₂
YM-22, 258	Densely welded, with vapor phase	C ₆	C ₂ -C ₇
YM-26, 323	Densely welded, with vapor phase	C ₅₋₆	C ₄ -C ₇
YM-30, 385	Vitrophyre, with minor vapor phase	C ₅	C ₂ -C ₇
YM-31, 390	Vitrophyre, with minor vapor phase	C ₇	C ₇
YM-35, 421	Zeolitized, nonwelded ash-flow tuff	C ₆	C ₅ -C ₇

USW-G1 Samples Not Described in G1 Report

Sample Depth (in m)	Rock Description	Oxidation States	
		Average	Range
89	Moderately to densely welded, with minor vapor phase	C ₃	--
137	Moderately welded, with vapor phase	C ₆	C ₁ -C ₆
154	Moderately to densely welded, with vapor phase	C ₆	C ₁ -C ₇
189	Densely welded, with vapor phase	C ₅₋₆	C ₃ -C ₇
220	Densely welded, with minor(?) vapor phase	C ₂₋₃	C ₁ -C ₆
231	Moderately to densely welded, with vapor phase	C ₅	C ₂ -C ₇

series of densely to moderately welded ash-flow tuffs. Characteristically, the moderately welded tuffs form the top of the lower cooling unit. The moderately welded zone of this lower cooling unit is much less evident and tends toward dense welding in the G1 core. Various possibilities are that the moderately welded zone was stripped off by erosion, or that the G1 locale was sufficiently near the cauldron source to retain a high temperature and allow dense welding throughout.

Devitrification, vapor-phase, and alteration products also correlate to a large degree between the two cores of the Topopah Spring Member. The zeolitized nonwelded tuffs (at the base of the lower cooling unit) and zeolite fracture fill in the lower vitrophyre are primarily clinoptilolite + mordenite and heulandite, respectively, in UE25a-1. In the G1 section, clinoptilolite is the only zeolite observed in the former environment (no mordenite). This minor zeolite phase variation between drill cores can most probably be ascribed to variations in ground-water chemistry. Immediately above the lower vitrophyre, both cores show densely welded devitrified tuffs that are devoid of vapor-phase crystallization. The two sections of Topopah Spring also share the same primary devitrification and vapor-phase crystallization in the densely welded devitrified tuffs (quartz-lathite caprock), and an overlying non-altered vitrophyre.

B. Lithic-Rich Tuff

The Lithic-rich tuff has been described in the G1 report. Further study of the Lithic-rich tuff by additional microprobe and thin-section analyses has not substantially changed the description found in the G1 report of that unit. There were no significant questions with regard to that report concerning the lithic fragments, opaque mineral oxidation states, degree of welding, phenocryst abundance or compositions, etc. Of importance are the type and abundance of low-grade metamorphic alterations, specifically involving the minerals analcime, albite, sericite, chlorite, calcite, and also the alteration of feldspar phenocrysts. Questions also arose about the possibility of undiscovered high-temperature zeolites such as wairakite and laumontite and/or the presence of prehnite-pumpellyite facies minerals as constituents of the Lithic-rich tuff. No such minerals had been reported in the earlier x-ray analyses of these samples (Bish et al. 1981), but minor amounts could have escaped detection.

No significant previously undiscovered authigenic minerals were found within the Lithic-rich tuff, although some phases reported here were not discussed in the G1 report. Thorough study of the thin sections showed several occurrences of unrecognized phases (low-birefringent), but subsequent microprobe analysis showed them to be either alkali feldspar (sanidine or anorthoclase), silica, or nearly pure authigenic potassium feldspar. The first occurs as more or less fragmental-appearing, fibrous, spherulitic or radial aggregates, often with threadlike, branching crystals (rutile?) parallel to the fibrous structure. The second was generally identified as chalcedony in thin section (spherulitic/botryoidal, low birefringence), and the third occurs as tabular, untwinned, clear crystals generally projecting into void spaces and having a dark gray birefringence. For microprobe results, see Table VI.

TABLE VI.
COMPOSITIONS OF THREE UNKNOWN PHASES IN THE LITHIC-RICH TUFF
AS DETERMINED BY MICROPROBE ANALYSIS^a

Oxides	Radiating Fibrous Aggregates			Unknown Phases Chalcedony(?)			Tabular Dark Gray Crystals	
	Na ₂ O	8.50	10.11	5.26	0.34	0.14	0.18	0.02
Al ₂ O ₃	18.83	19.34	18.56	7.36	5.22	5.52	17.17	17.19
SiO ₂	68.16	68.46	67.70	87.65	90.82	91.77	68.88	67.50
BaO	0.00	0.02	0.13	0.02	0.11	0.03	0.09	0.00
FeO	0.37	0.57	0.66	0.22	0.00	0.78	0.00	0.01
K ₂ O	3.57	1.49	8.26	5.15	3.59	2.34	15.30	15.33
CaO	0.49	0.58	0.45	0.43	0.08	0.13	0.02	0.01
TOTAL	99.91	100.56	101.02	101.17	99.96	100.74	101.48	100.06
	<u>Sample Depths (in m)</u>							
	1372	1464	1614 ^b	1309	1486	1497	1486	1497

^a Each list of oxide weight percents is an average of a few analyses for one occurrence of the unknown in the thin section.

^b Sample is from below the Lithic-rich tuff but is the only occurrence that does not look fragmental.

The Lithic-rich tuff extends from 1203 to 1506 m in the USW-G1 core and is composed of two units: an upper ash-flow tuff (297 m thick) and a lower bedded tuff (5.8 m). No samples were taken of the bedded tuff, but twelve samples of the ash flow were examined in thin section. These samples were taken at 1218, 1248, 1282.5, 1309, 1323, 1341, 1372.5, 1406, 1432.5, 1464.5, 1486, and 1497 m.

The description in the G1 report of the authigenic crystallization in the Lithic-rich tuff needs revision only regarding the extent of the alterations. The general picture of alteration is still applicable. Revised descriptions of the Lithic-rich tuff are:

- (1) Analcime is a significant pseudomorph of pumice, although analcime is altered to varying extents in all samples of the ash flow.
- (2) Optically recognizable albite is rare or absent in the samples at 1372.5, 1406, 1432.5, and 1464.5 m. It is obvious at 1309, 1323, and 1341 m, and again at 1486 and 1497 m.
- (3) Starting at 1341 m and continuing down through the ash flow, chalcedony is an important phase.
- (4) Sericite and chlorite are present in varying amounts throughout the ash flow.
- (5) Feldspar phenocrysts can be moderately altered (usually sericitized) in the Lithic-rich tuff and do show overgrowths, especially in the deeper samples.
- (6) Calcite is not generally a void-fill but occurs as a late-stage patchy replacement of various components of the rock.

Throughout the Lithic-rich tuff ash-flow sequence, analcime is a common replacement of pumice fragments and the dominant replacement phase of shards. In analcime-pseudomorphed pumice fragments, the most typical alteration is to strands of sericite and/or clay. Generally, within one thin section, pumice fragments vary from completely analcime to strongly sericitized, but alteration is generally minimal at 1282.5, 1309, and 1341 m, and extensive at 1248, 1406, and 1432.5 m. In samples below 1400 m (roughly), other alteration minerals are present in analcime-pseudomorphed pumice fragments, such as calcite, chalcedony, and albite.

Shards (pseudomorphed by analcime) are much less altered than pumice fragments throughout the ash flow. With the exception of the samples at 1282.5 and 1323 m, analcimitized shards are generally replaced only along their

boundaries by the same minerals recrystallizing the groundmass—chalcedony or albite. In the two exceptions, some analcimitized shards are recrystallized, either completely or partially, to a mixture of clay and/or sericite with or without silica.

Sericite and chlorite are present in all thin sections of the Lithic-rich tuff in varying amounts. Thin, diffuse, wandering strands of sericite are typically present in pumice fragments pseudomorphed by analcime and are also present in the groundmass. Tiny single crystals of sericite and chlorite are typically finely disseminated through the groundmass. In many samples, sericite mixed with minor chlorite forms veinlets; these are especially thick in the samples at 1218 and 1486 m. These veinlets frequently contain crumpled biotite, sheared or offset along cleavage planes, and a few veinlets might have formed by collapse of pumice fragments. Chlorite is noticeably concentrated around large opaque oxides in many sections. Because the groundmass has tiny disseminated opaque minerals in many sections, associated chlorite may be similarly disseminated.

Alteration products can occasionally be seen to develop throughout the groundmass, but often the groundmass is too fine grained to enable identification of either its original or its present constituents. This is certainly true of the samples at 1218 and 1248 m. Clays and opaque oxides (and chlorite and sericite?) are disseminated throughout, but minerals forming a microcrystalline component in the groundmass could not be precisely identified. Through the succeeding samples at 1282.5, 1309, 1323, and 1341 m, the groundmass becomes progressively brighter under crossed nicols, changing from gray to gray-white birefringence, and it also becomes coarser grained with depth through the latter three samples. In those same three samples, tabular or lathlike crystals of albite, mostly projecting into voids, are present. First seen at 1309 m, they become larger and more abundant through the next two samples. In the sample at 1341 m, the climax of this albitization trend, plagioclase crystals can finally be seen in the groundmass. Interestingly, in this same sample, when the edges of shards are observed closely, botryoidal forms (probably chalcedony) are seen edging the analcime in addition to crystals more likely to be albite.

In the next three deeper samples (at 1372.5, 1406, and 1432.5 m), the groundmass is once again dark and very fine grained, high in clays and oxides, but chalcedony is a significant part of the groundmass. Albite is not

observed in voids or groundmass, but potassium-feldspar crystals (see Table VI) are present in voids. Chalcedony becomes coarser grained and more abundant (and obvious) in the groundmass of samples from 1432.5 to 1497 m. However, in the last two samples, at 1486 and 1497 m, albite crystals once more fill voids. In the former sample, plagioclase phenocrysts in contact with analcime have obvious overgrowths only into the analcime, into which they project with euhedral terminations. The groundmass, however, is still dominated by chalcedony, seemingly to the exclusion of albite, although the latter mineral may simply be too fine grained to be resolved optically.

The description in the G1 report of feldspar phenocrysts in the Lithic-rich tuff suggests greater breakdown of them than actually is the case. Sericitization is the dominant alteration, is generally only moderate, and certainly not uniform. Overgrowths on feldspars occur to a minor extent in samples generally below 1341 m, but, as indicated previously, they achieve their most obvious metamorphic significance only in the deepest two samples.

Starting at 1282.5 m and continuing through the ash flow of the Lithic-rich tuff, calcite alteration and minor void-fill is present in the thin sections. Generally the calcite occurs in minor, isolated patches but in those patches replaces nearly everything. The calcite becomes erratically more abundant with depth and is most abundant at 1486 m. Generally there seems to be little preference as to alteration locale, but deeper in the core, analcime is frequently replaced by calcite, as are areas of shards and groundmass.

In summary, albite, chlorite, sericite, and quartz are developed throughout the Lithic-rich tuff in the USW-G1 core. Since the albite can be demonstrated to have formed from analcime (Bish et al. 1981), Iijima's (1975) Zone III has been surpassed, and the Lithic-rich tuff represents the beginning of Iijima's Zone IV. The mineralogic transitions, however, do not overwhelm the rock. Instead, analcime is a prominent metastable phase as a pseudomorphing mineral of shards and pumice fragments through all the thin sections of the ash flow, and the development of albite is sporadic and may be volumetrically minor. Only toward the bottom of the ash flow does the transition out of Zone III seem to become dominant.

IV. SUMMARY AND CONCLUSIONS

Petrologic descriptions of the Topopah Spring Member of the Paintbrush Tuff and the Lithic-rich tuff have been expanded to be comparable with

descriptions of other possible radioactive waste isolation repository horizons (at Yucca Mountain, NTS). The Topopah Spring Member was compared between drill cores from UE25a-1 and USW-G1 and found to be extremely similar in both cores. Questions that arose in the G1 report concerning the Lithic-rich tuff have been addressed and no major changes have resulted.

Clays are found to be ubiquitous throughout all the samples analyzed in this report. Zeolites are present in all Lithic-rich tuff samples and in the nonwelded basal portion and lower vitrophyre fracture fill of the Topopah Spring Member. In addition, the ubiquitous clays and zeolites encountered in the horizons studied all have limited thermal stabilities and are greatly affected by varying water pressures.

In addition, an extremely thick sequence of lithophysal cavities occurs in the moderately to densely welded portions of the Topopah Spring Member. A sequence of lithophysal cavities such as is seen in the Topopah Spring will undoubtedly have direct consequences on physical rock properties. The high incidence of large and small fractures in this zone will affect the possibility of water transport.

Therefore, the following factors that have been encountered must be addressed before any horizon can be accepted as a possible waste repository horizon.

- (1) What are the physical and mechanical rock properties of a thick zone containing lithophysal cavities?
- (2) How would hydrologic transport be affected by such a lithophysal zone?
- (3) Are the abundant fractures of the lithophysal zone filled with stable minerals?
- (4) What are the phase stabilities of the zeolites and clays encountered in the Topopah Spring and in the Lithic-rich tuff? How do temperature and water pressure affect phase transformations and/or degradations, and how do these changes correlate to possible volume, permeability, porosity, net water, and mechanical property variations in possible repository horizons?

REFERENCES

- Bish, D. L., F. A. Caporuscio, J. F. Copp, B. M. Crowe, J. D. Purson, J. R. Smyth, and R. G. Warren, "Preliminary Stratigraphic and Petrologic Characterization of Core Samples from USW-G1, Yucca Mountain, Nevada," Los Alamos National Laboratory report LA-8840-MS (1981).
- Haggerty, S. E., "Oxidation of Opaque Mineral Oxides in Basalts," in Oxide Minerals, Min. Soc. Amer. Short Course Notes 3, H6-1 - H6-100 (1976).
- Iijima, A., "Effect of Pore Water to Clinoptilolite - Analcime - Albite Reaction Series," J. Fac. Sci. Univ. Tokyo, Sec. II 19, 133-147 (1975).
- Lipman, P. W., R. L. Christiansen, and J. T. O'Connor, "A Compositionally Zoned Ash-Flow Sheet in Southern Nevada," US Geol. Surv. Prof. Paper 524-F, F-1 - F-47 (1966).
- Reynolds, R. C. and J. Hower, "The Nature of Interlayering in Mixed-Layer Illite-Montmorillonites," Clays and Clay Minerals 18, 25-36 (1970).
- Spengler, R. W., F. M. Byers, Jr., and J. B. Warner, "Stratigraphy and Structure of Volcanic Rocks in USW-G1, Yucca Mountain, Nye County, Nevada," US Geol. Surv. Open-File Report (in preparation).
- Spengler, R. W., D. C. Muller, and R. B. Livermore, "Preliminary Report on the Geology and Geophysics of Drill Hole UE25a-1, Yucca Mountain, Nevada Test Site," US Geol. Surv. Open-File Report 79-1244, 43 p. (1979).
- Sykes, M. L., G. H. Heiken, and J. R. Smyth, "Mineralogy and Petrology of Tuff Units from the UE25a-1 Drill Site, Yucca Mountain, Nevada," Los Alamos Scientific Laboratory report LA-8139-MS (1979).

865

Box 2

865

LA-9021-MS

UC-11

Issued: October 1981

**Detailed Mineralogical Characterization
of the Bullfrog and Tram
Members in USW-G1, with Emphasis
on Clay Mineralogy**

David L. Bish

Los Alamos Los Alamos National Laboratory
Los Alamos, New Mexico 87545

DETAILED MINERALOGICAL CHARACTERIZATION OF THE BULLFROG AND TRAM MEMBERS
IN USW-G1, WITH EMPHASIS ON CLAY MINERALOGY

by

David L. Bish

ABSTRACT

The detailed mineralogy of the Bullfrog and Tram Members of the Crater Flat Tuff from drill hole USW-G1 has been examined, primarily to characterize fully the amounts and types of clay minerals in the tuffs and the possible effects clay minerals have on rock properties. Results of bulk sample x-ray diffraction analyses agree closely with previous determinations, although slightly higher clay mineral contents were found in this study. X-ray diffraction analysis of fine fractions revealed that the clay minerals in the tuffs are sodium-saturated montmorillonite-beidellites with typical layer charges and no high-charge layers. These smectites are found in virtually all samples of the Bullfrog and Tram, and there is no correlation between the amounts of smectites and the amounts of zeolite, quartz, and feldspar. Smectites are present in both welded and nonwelded horizons and are scarce in some zones with slight-to-absent welding. The montmorillonite-beidellites are all randomly interstratified with a small amount (about 10%) of illite, and there is no consistent trend in the degree of interstratification with depth, contrary to what is commonly found in pelitic sediments. This observation, together with the lack of smectites in some zeolitized zones, suggests that clay mineral formation occurred after zeolite crystallization and under conditions similar to those in the rocks today (35-45°C). It is also likely that the ground water in the tuffs has inhibited the smectite-to-illite reaction.

The montmorillonite-beidellites exist in a 12.6 Å form under room conditions, and their basal spacings can range from 10 Å at 0% relative humidity or slightly elevated temperatures to approximately 20 Å in a 100% relative humidity atmosphere. Further increases in water:clay ratio cause additional expansion. In view of the possible significant variations in montmorillonite-beidellite molar volume and water content with small changes in temperature and relative humidity, it is important that we understand the present conditions existing in the rocks and appreciate the changes

in rock and mineral properties expected when altering these conditions, either in a repository or in a laboratory test.

I. INTRODUCTION

The tuffs of the Nevada Test Site (NTS) region have been and are currently under investigation as repository media for high-level radioactive waste. Under these studies, a detailed exploration program began in 1979 at Yucca Mountain, and several exploration holes were drilled. Data from the drill holes UE25a-1 and USW-G1, including geophysical, stratigraphic, structural, and petrographic information, are reported by Sykes et al. (1979), Spengler et al. (1979, in preparation), Bish et al. (1981), and Carroll et al. (1981). Bish et al. (1981) concluded that four horizons in the USW-G1 hole have favorable characteristics for a waste repository: the lower cooling unit of the Topopah Spring Member of the Paintbrush Tuff; the lower cooling unit of the Bullfrog Member of the Crater Flat Tuff; the Tram Member of the Crater Flat Tuff (Spengler et al. in preparation); and the Lithic-rich tuff (Spengler et al. in preparation). The latter unit has been tightly sealed by recrystallization during burial metamorphism, and the three other units contain thick densely welded and zeolite-free horizons.

Carroll et al. (1981) focused on the details of the Topopah Spring Member of the Paintbrush Tuff and the Lithic-rich tuff and included a discussion of the clay mineralogy in the Topopah. They found that interstratified montmorillonite/illites were ubiquitous throughout the Topopah in hole UE25a-1, occurring in both welded and nonwelded horizons in amounts ranging from several per cent to approximately 20%. There was little variation in the degree of interstratification, and all of the clays examined were at least 80% smectitic (swelling). Optical petrographic examination demonstrated that the clays occurred in the groundmass and were concentrated along shard boundaries and pumice tube walls. Bish et al. (1981) reported the detailed petrography and mineralogy of the USW-G1 core, but they presented only a preliminary discussion of the clay mineralogy. Selected samples from the Bullfrog and Tram Members contained dioctahedral smectites randomly interstratified with less than 20% illite.

Because the data presented by Bish et al. (1981) concerning the clay mineralogy of the Bullfrog and Tram Members were of a preliminary nature, it is the purpose of this report to describe the clay mineralogy in detail and to briefly discuss the possible effects of clays on rock properties. Although clay minerals are commonly present in low concentrations within the tuffs at Yucca Mountain, they are ubiquitous and can profoundly affect element sorption, rock strength, and the porosity and permeability of tuff. Erdal et al. (1980) and Smyth et al. (1980) emphasize that it is possible for a minor phase to completely dominate the sorption properties of a rock, and the results of Smyth et al. (1980) suggest that clay minerals control sorption in granites. The numerous papers in Longstaffe (1981) demonstrate the very important effect clay minerals, especially swelling clays, have on rock porosity and permeability. Minor changes in temperature and ground-water chemistry can dramatically lower the porosity and permeability. Finally, as a result of the swelling nature of smectites, small changes in temperature, pressure, and humidity can release water and lead to major volume changes. Because the clay minerals in the tuffs can have such a substantial effect on the chemical and mechanical behavior of the rocks, it is essential to examine the mineralogy in detail and to elucidate the effects of temperature and humidity on the clay minerals. For the present work, most samples examined in Bish et al. (1981) have been studied, and an additional suite of samples has been collected and examined. Because large samples were used in the clay mineral separations, x-ray diffraction patterns of homogeneous bulk samples were obtained routinely before performing the clay mineral separations.

II. STRATIGRAPHY

The stratigraphy of the Bullfrog and Tram Members in USW-G1 has been described in detail by Spengler et al. (in preparation) and Bish et al. (1981), and only a brief description of these units will be presented here. The stratigraphic position of the Bullfrog and Tram Members in USW-G1 is shown in Fig. 1. The Bullfrog Member of the Crater Flat Tuff is approximately 144 m thick and is composed of two major units, an upper unit (BF-I) containing two tuff sheets and a lower unit (BF-II) containing five different tuff sheets. These two units are separated by a thin bedded tuff. The BF-I is nonwelded and is composed of two ash flows that appear to have cooled as a single unit. The

YUCCA MOUNTAIN GEOLOGIC UNITS

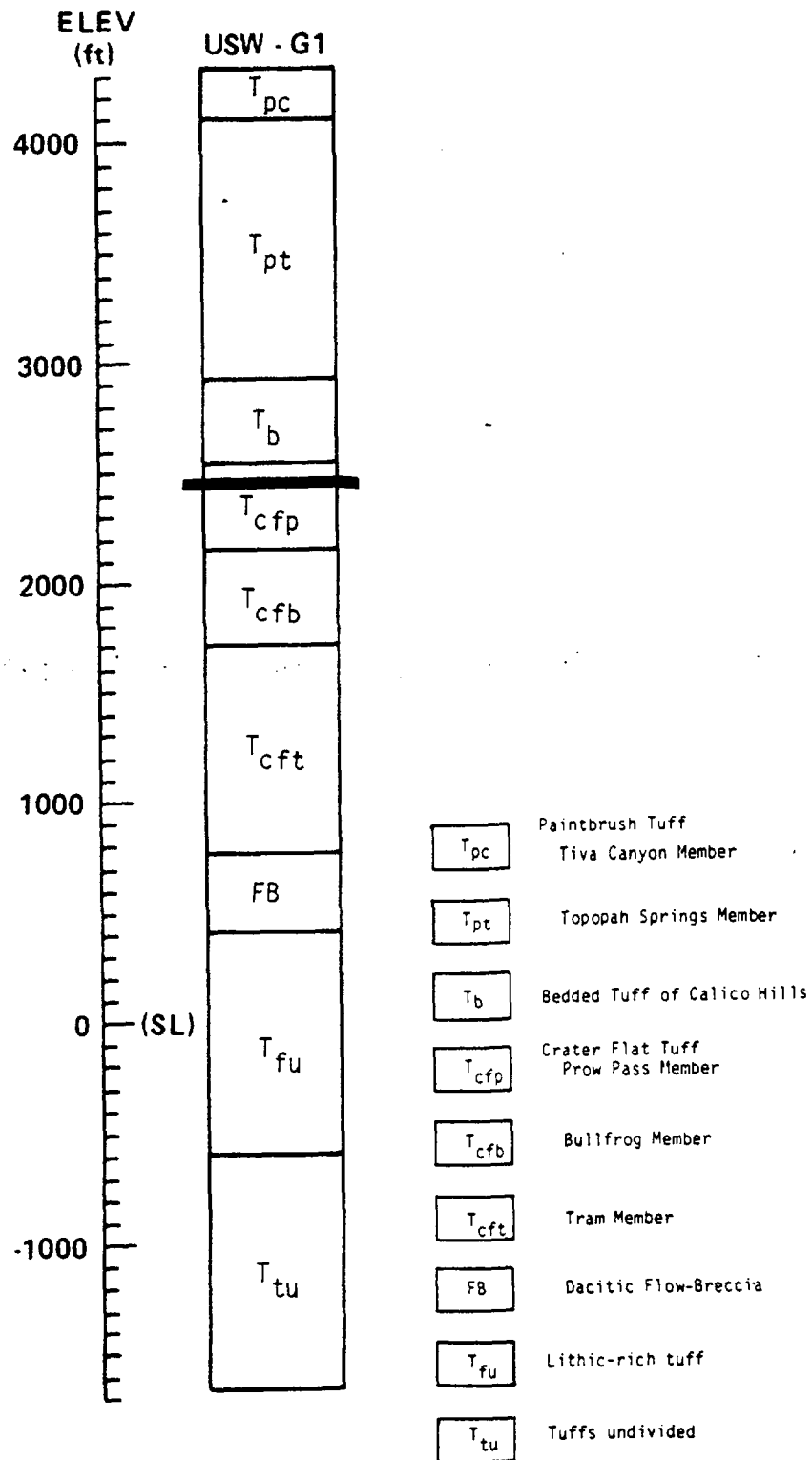


Fig. 1.

Stratigraphic column for drill hole USW-G1 showing the positions of the Bullfrog and Tram Members. The heavy black line is the static water level in the hole.

BF-II is a single cooling unit ranging from slightly welded at the top and bottom to moderately welded within the interior.

In BF-I, all glass shards are pseudomorphed by zeolites, and clays are slightly more abundant in the groundmass than in BF-II. Zeolites also replace glass shards and fill void spaces in the bottom of BF-II, reflecting the absence of welding and original high permeability. Above the zeolitized section of BF-II, the degree of welding increases and the alteration phases decrease in abundance, reflecting the decreased permeability in the central and upper sections of BF-II.

The Tram Member of the Crater Flat Tuff is composed of five units, a basal bedded tuff and four ash-flow sheets. Petrographically, the Tram can be divided into two units, an upper, single, largely devitrified cooling unit, and a lower unit composed of three ash flows and a reworked tuff. The upper unit is zeolitized near the top and has a densely welded lower portion showing devitrification to quartz and alkali-feldspar. The lowermost ash flow in the lower Tram exhibits the transition from clinoptilolite to analcime (Bish et al. 1981). The second ash-flow unit of the lower Tram is nonwelded, zeolitized, and oxidized. The uppermost ash-flow unit of the lower Tram is partially welded and is zeolitized.

III. REVIEW OF SMECTITE MINERALOGY

Smectites very commonly form as alteration products of volcanic rocks, including tuffs and volcanic ash, and montmorillonite can form from clinoptilolite (Ames et al. 1958). The term smectite is used as a group name for the swelling 2:1 clay minerals including montmorillonite, beidellite, nontronite, saponite, hectorite, and saucnite (Brindley et al. 1975; Table I, Deer et al. 1966). All smectites possess a structure similar to talc or pyrophyllite, with ionic substitutions creating negatively charged layers (Fig. 2). The silicate layers are composed of an octahedral sheet between two tetrahedral sheets; thus the notation 2:1 layer silicates. Octahedral sheets can have either two out of three or three out of three octahedral sites occupied yielding, respectively, dioctahedral or trioctahedral layers. The negative charge on the 2:1 layers can arise through the substitution of aluminum for tetrahedral silicon and/or the substitution of magnesium for octahedral aluminum. In the smectites, cations are present between the layers to balance the negative charge on the 2:1 layers; these "interlayer cations" may include

TABLE I
IDEALIZED SMECTITE, PYROPHYLLITE, AND TALC COMPOSITIONS

	<u>Diocahedral</u>		
	<u>Z</u>	<u>Y</u>	<u>X</u> (exchange cations)
Pyrophyllite	Si ₈	Al ₄	--
Montmorillonite	Si ₈	Al _{3.34} Mg _{0.66}	(1/2Ca,Na) _{0.66}
Beidellite	Si _{7.34} Al _{0.66}	Al ₄	(1/2Ca,Na) _{0.66}
Nontronite	Si _{7.34} Al _{0.66}	Fe ₄ ⁺³	(1/2Ca,Na) _{0.66}
	<u>Triocahedral</u>		
Talc	Si ₈	Mg ₆	--
Saponite	Si _{7.34} Al _{0.66}	Mg ₆	(1/2Ca,Na) _{0.66}
Hectorite	Si ₈	Mg _{5.34} Li _{0.66}	(1/2Ca,Na) _{0.66}
Sauconite	Si _{6.7} Al _{1.3}	Zn ₄₋₅ (Mg,Al,Fe ⁼³) ₂₋₁	(1/2Ca,Na) _{0.66}

any of the alkali or alkaline earth cations. The compositions of smectites are such that their negative layer charge is low, approximately -0.33 per Si₈O₂₀(OH)₄ formula unit. This compares with layer charges of about -0.66 for vermiculites, -1.0 for micas, and -2.0 for brittle micas.

Because the electrostatic attraction between layers is small and the interlayer cations interact with water, smectites can expand in a direction perpendicular to the layers. The exact nature of the expansion in water is thus related to the type of interlayer cation (for example, charge, size, hydration energy) and, depending on conditions, smectites can have layer thicknesses ranging from 10 Å to > 20 Å. An additional consequence of the weak interlayer attraction and hydrated interlayer cations is the phenomenon of cation exchange. Smectites typically have cation exchange capacities ranging from 70 to 130 meq/100 g of clay, and sodium, calcium, magnesium, and hydrogen are the most common interlayer cations (Weaver et al. 1975). Large univalent cations such as potassium and cesium can be "fixed," that is, irreversibly exchanged, onto smectites with above average layer charge if the interlayer attraction

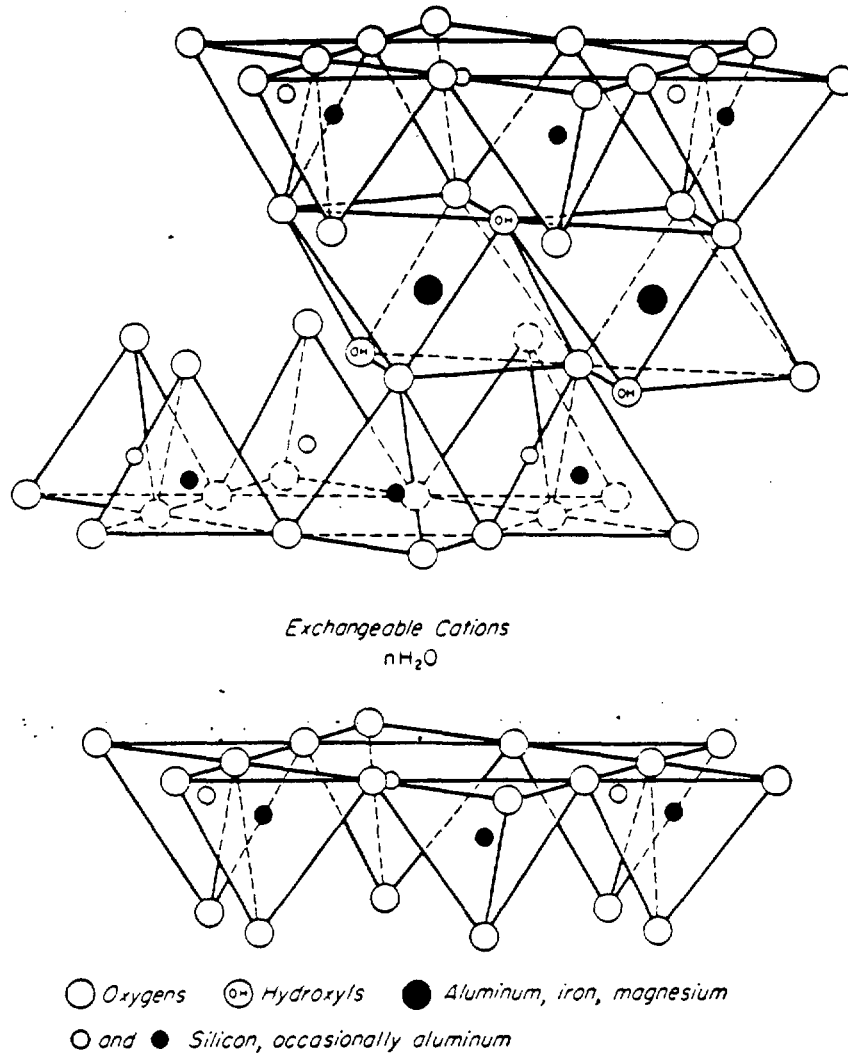


Fig. 2.
Diagrammatic sketch of the structure of montmorillonite (after Grim 1953).

exceeds the cation hydration energies. Cation fixation thus occurs more readily in high-charge smectites or those containing scattered high-charge layers. In addition, divalent cations are generally preferred in exchange reactions over univalent cations of similar hydrated size.

Numerous authors (Burst 1959; Perry et al. 1970, 1972) have shown that smectites undergo a transition to a mica-like mineral with increasing depth or temperature. This reaction involves both compositional and structural changes; there is a gain in interlayer potassium and additional substitution of aluminum for silicon in the tetrahedral layers, thereby increasing the net

cation exchange capacity gradually decreases from values typical of pure smectites to approximately 15 meq/100 g, and the amount of swelling in water and organic liquids is gradually reduced. Ormsby et al. (1954) demonstrated that a linear relation exists between the cation exchange capacity and per cent expandable layers in illites and interstratified illite/smectites.

IV. EXPERIMENTAL METHODS

The investigation of samples in this work involved standard x-ray powder diffractometer techniques and examination of clays separated by sedimentation and centrifugation. Bulk samples were crushed to approximately -300 mesh and mounted in cavities in glass slides. The cavities were large enough so that the sample area fully contained the x-ray beam at the lowest angle of interest. This technique ensured that clay mineral contents in the bulk samples would not be underestimated. Relative percentages of the different phases were determined by comparison with standard patterns.

More accurate clay mineral identification involved first dispersing the crushed bulk samples in distilled water in an ultrasonic bath. The large size fraction (greater than 10 μm) was sedimented out and a finer fraction was obtained via centrifugation. Through x-ray analysis of the fine fraction, it is possible to identify very small amounts of clay minerals. Oriented sample mounts were prepared for x-ray diffraction by dropping an aqueous suspension of the fine fraction onto a glass slide and allowing it to dry. These mounts were then x-rayed after the following treatments: (1) air dried, 30% relative humidity, (2) dried at 100°C for at least 6 h, (3) ethylene glycol solvation, (4) heated to 200°C with subsequent ethylene glycol solvation, and (5) solvation with water. In addition, the fine fraction from G1-3500 was saturated with lithium and potassium in LiCl and KCl solutions, heated to 200°C, and solvated with ethylene glycol.

Heating a lithium-saturated smectite fixes the lithium into available interlayer and octahedral vacancies and is useful in distinguishing between tetrahedral and octahedral charge deficiencies in smectites (Greene-Kelley 1955). Dioctahedral smectites with octahedral charge deficiencies (montmorillonites) will not expand in ethylene glycol after lithium saturation and heating. Smectites with the layer charge originating in the tetrahedral sheet (beidellites) will expand to approximately 16.9 Å after lithium saturation and heating. Potassium saturation of smectites yields information on the

magnitude of the layer charge deficiencies. Expandable layers with sufficiently high negative charge will collapse to 10 Å after potassium saturation.

The air dried, 100°C dried, and water solvated samples provide information on the type of interlayer cation present and on the behavior of the clay with changes in temperature and humidity. Sodium-saturated smectites commonly exhibit basal spacings of approximately 19.5, 15.6, 12.6, and 10 Å with decreasing humidity, demonstrating the existence, respectively, of three, two, one, and no layers of water between the smectite layers. Calcium- and magnesium-saturated smectites exist predominantly in the two-layer hydrate form (14-15 Å), and potassium smectites occur in 10 Å (no-water layers) and 12.6 Å (one-water layer) forms (Gillery 1959; Suquet et al. 1975).

The x-ray patterns of ethylene-glycol-solvated smectites provide additional useful information. Solvation of smectites with ethylene glycol produces a stable complex yielding more easily interpretable x-ray patterns. Using the methods of Reynolds et al. (1970) and Srodon (1980) and comparing the observed x-ray patterns to hypothetical patterns calculated for a given type of interstratification, it is possible to determine accurately the presence and nature of interstratification. Figure 4 illustrates the calculated changes that take place in the diffraction patterns going from pure smectite through randomly interstratified smectite/illite to pure illite.

V. RESULTS AND DISCUSSION

Bish et al. (1981) described the bulk mineralogy of the Bullfrog and Tram Members from core samples from USW-G1. However, because several additional samples of core were obtained and because large homogeneous samples were required for the clay mineral separations, I repeated bulk sample x-ray diffraction analyses (Table II).

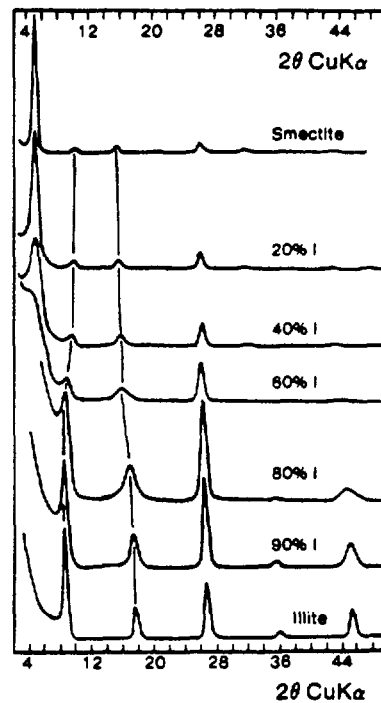


Fig. 4. $(00\ell)_I/(00\ell)_S$ diffraction profiles of randomly interstratified illite/glycol-smectite. Lines connect the $(001)_{10}/(002)_{17}$ and $(002)_{10}/(003)_{17}$ combined reflections (Hower 1981).

TABLE II
X-RAY DIFFRACTION ANALYSIS OF BULK SAMPLES OF THE BULLFROG
AND TRAM MEMBERS FROM USW-G1

SAMPLE	(m)	Smectite	Mica	Clinop- tilolite	Mordenite	Analcime	Quartz	Cristo- balite	Alkali Feldspar
G1-2176	663.2	<5%	5-10	30-50	5-15	--	5-10	5-20	15-30
G1-2198	670.0	5-15	5-10	50-70	--	--	--	5-15	10-20
G1-2247	684.9	<5%	~5	40-60	5-15	--	10-20	5-15	20-40
G1-2318	706.5	15-30	10-20	--	--	--	10-20	--	50-70
G1-2349	716.0	~5	~5	--	--	--	30-50	--	40-60
G1-2436	742.5	5-10	~5	--	--	--	30-50	--	40-60
G1-2467	751.9	<5	~5	--	--	--	30-40	5-15	40-60
G1-2486	757.7	<5	5-10	--	--	--	30-50	--	40-60
G1-2525	769.6	<5	<5	--	--	--	30-50	--	40-60
G1-2555	778.8	<1	<5	25-45	25-45	--	5-10	10-20	10-20
G1-2587	788.5	<1	5-10	30-50	30-50	--	--	5-10	5-15
G1-2600	792.5	--	5-10	25-45	15-35	--	5-10	--	10-30
G1-2613	796.4	<5	~5 ^a	<5	20-40	--	20-40	~5	30-50
G1-2622	799.2	<5	5-10	20-40	10-20	--	20-40	<5	20-40
G1-2633	802.5	~5	5-10	30-50	15-30	--	20-40	5-10	5-15
G1-2641	805.0	5-10	10-20	20-40	--	--	10-20	5-20	25-40
G1-2715	827.5	~5	~5	30-50	--	--	10-20	10-30	10-20
G1-2748	837.6	~5	~5	5-15	<5	--	20-40	10-30	20-40
G1-2781	847.7	5-10	~5	--	--	--	40-60	5-10	30-50
G1-2804	854.7	<5	5-10	--	--	--	40-60	0-10	40-60
G1-2820	859.5	5-10	<5 ^a	--	--	--	40-60	--	40-60
G1-2868	874.2	<5	5-10	--	--	--	30-50	--	40-60
G1-2884	879.0	<2	~5	--	--	--	40-60	--	40-60
G1-2932	893.7	<2	~5	--	--	--	40-60	--	40-60
G1-2981	908.6	<2	~5	--	--	--	40-60	--	40-60
G1-3001	914.7	5-10	~5	--	--	--	40-60	--	40-60
G1-3039	926.3	<2	5-10	15-30	5-15	--	30-50	--	20-40
G1-3099	944.6	5-10	5-15	15-30	--	5-10	30-50	--	20-40
G1-3137	956.2	5-15	5-10	--	<5	5-15	25-45	--	15-35
G1-3196	974.1	5-10	~5	10-20	<5	<5	30-50	--	15-30
G1-3238	986.9	5-15	<5	10-20	--	<5	30-50	--	15-30
G1-3258	993.0	10-20	~5 ^a	10-20	--	--	25-45	--	20-40
G1-3321	1012.2	5-15	~5	5-15	--	<5	30-50	--	15-30
G1-3345	1019.6	5-15	~5	10-20	--	<5	20-40	--	25-45
G1-3371	1027.5	5-15	~5	--	--	10-20	30-50	--	30-50
G1-3468	1057.0	10-20	~5	5-15	--	<5	30-50	--	15-30
G1-3500	1066.8	15-30	~5	--	--	<5	30-50	--	15-30

^a Broad peak, possibly oxidized.

There are no major differences between these results and those presented in Bish et al. (1981), although Bish et al. commonly estimated lower smectite contents than I found in this study. This minor discrepancy is possibly due to differences in sample preparation technique; Bish et al. did not ensure that the full x-ray beam was contained within the sample area at low angles where the main smectite peak occurs. The results for the remaining phases are in excellent agreement.

All samples in the upper cooling unit of the Bullfrog Member (Bullfrog I) are zeolitized, and smectites are ubiquitous but in low concentrations. The upper portion of the Bullfrog II (706.5-769.6 m) is not zeolitized, but smectites are present in all samples. Clinoptilolite and mordenite are present in all lower samples of the Bullfrog II (778.8-802.5 m), however, unlike all other Bullfrog samples, there is a narrow range (778.8-792.5 m) in which smectites are virtually absent. Clinoptilolite is present in the upper portion (805.0-837.6 m) of the Tram, is absent from 847.7-914.7 m, and sporadically distributed throughout the remainder of the unit. Analcime first appears at 944.6 m and is present in all but one of the lower samples.

Smectites are present in all samples of the Tram examined here; the upper part (805.0-914.4 m) contains small amounts of smectites, but below 914.4 m, the Tram is fairly rich (up to 30%) in smectites. There are no consistent correlations in the Bullfrog and Tram Members between the amounts of smectites and the amounts of zeolites, quartz, and alkali feldspar. In some intervals, zeolitized zones are the poorest in smectite (Bullfrog), while in others (lower Tram), relatively abundant smectites and zeolites occur together. Smectites are present equally in welded and nonwelded horizons and, contrary to expectation, are scarce in some zones with absent or slight welding and probable high original permeability (Bullfrog Member, 762.0-792.5 m). The absence of smectites in nonwelded, zeolite-rich horizons may be due to lowering of permeability by zeolites. If so, this indicates that the formation of the smectites postdates zeolite growth in the tuffs.

Using the fine-fraction material separated from bulk samples, it is possible to identify the type of smectite and its reaction to changes in humidity and temperature. X-ray diffraction patterns of $< 2 \mu\text{m}$ material in cavity mounts yield an (06 ℓ) reflection from the smectites with a spacing of about 1.49 Å, very characteristic of the dioctahedral smectites montmorillonite and beidellite. Trioctahedral smectites typically have (06 ℓ) reflections at about

1.53 Å. The smectites in the Bullfrog and Tram Members are thus montmorillonite-beidellites. The fine-fraction from G1-3500 was lithium-saturated in an effort to distinguish between montmorillonite and beidellite. The sample was saturated, deposited on a glass slide, heated to 220°C, and ethylene-glycol solvated. The smectite still expanded to about 16.9 Å after this treatment, suggesting that the site of the negative charge is in the tetrahedral sheets and that the smectite is beidellite. However, the lithium-saturation test can yield incorrect results when heating samples on glass slides, possibly as a result of lithium-for-sodium exchange. (This information was discussed with D. Eberl in July, 1981). For this reason, and because the properties of montmorillonite and beidellite are so similar, I will refer to the clays in the Bullfrog and Tram as montmorillonite-beidellites.

Under room conditions (20-50% relative humidity, 20-25°C), all of the smectites examined have one layer of interlayer water yielding a basal spacing of approximately 12.6 Å. These conditions certainly do not represent those occurring in the rocks because both the Bullfrog and Tram Members are in the saturated zone with temperatures ranging from approximately 35 to 45°C (Bish et al. 1981). Solvating the montmorillonites with water and allowing them to dry while x-raying reveals that all of the montmorillonites examined expand to approximately 20 Å in a 100% relative humidity atmosphere and, as they dry, contract to approximately 12.6 Å, going through a 15 Å intermediate state. The behavior of these montmorillonites is typical of sodium-saturated smectites and is depicted by Fig. 5 (Gillery 1959; Suquet et al. 1975). There are, however, minor fluctuations in the spacings of the different hydrates, probably because of variations in layer charge and interlayer cation. Depending on the exact conditions present in the rocks, the montmorillonites can have a large variation in basal spacing and consequently in molar volume. As stated above, from 0 to 100 % relative humidity, the basal spacings vary from 10 Å to approximately 20 Å, and the swelling pressure is approximately 4×10^9 dyne/cm² (Norrish, 1972). With increasing water content (g water/g clay), sodium-montmorillonites become plastic and disperse in a manner depicted in Fig. 6. The swelling pressure in the plastic region (region 2) is from 10^5 - 10^7 dyne/cm². Finally, with additional water (> 20 g water/g clay), sodium-montmorillonites disperse completely with a swelling pressure of $< 10^5$ dyne/cm². Obviously, knowing the natural hydration state of the montmorillonites is very important in understanding the effects of changing conditions

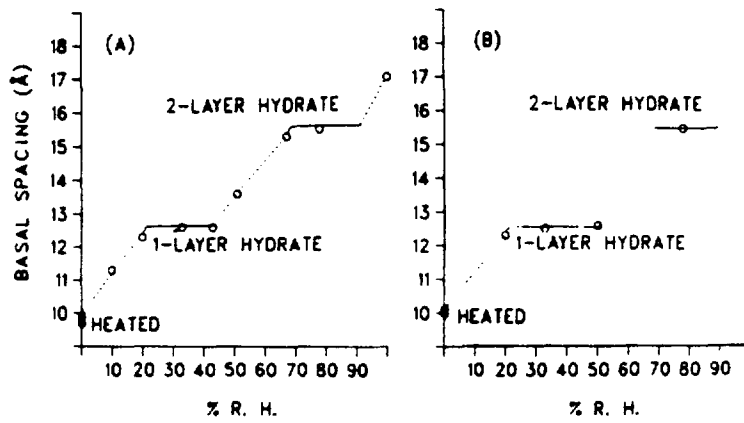


Fig. 5.

Basal-spacing relative-humidity relations (R. H.). (a) Natural sodium-montmorillonite, (b) synthetic sodium-beidellite (after Gillery 1959).

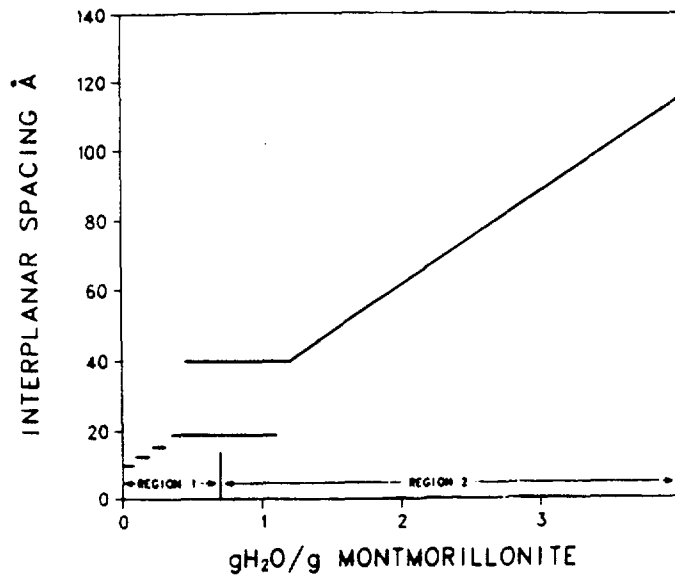


Fig. 6.

Swelling of sodium-montmorillonite (after Norrish 1972).

on the montmorillonites and ultimately on rock properties. It is thus imperative that we understand the present conditions existing in the rocks and appreciate the changes in rock and mineral properties expected when altering these conditions, either in a repository or in a laboratory test.

Further information on the behavior of the montmorillonite-beidellites when heated can be obtained by heating samples to 200°C and re-solvating with ethylene glycol. Samples with high-charge layers and appreciable interlayer potassium will expand only partially, or not at all, after this treatment. Sample G1-3196 was the only sample to be affected by heating, only partially expanding in ethylene glycol. Heating this sample to 100°C had no effect on the expansion behavior. In addition, potassium saturating and heating the montmorillonite-beidellite in G1-3500 had no effect on the expansion properties. The montmorillonite-beidellites in the Bullfrog and Tram Members have typical layer charges (about 0.33) and few or no high-charge layers. This suggests that the cation exchange capacities will not be substantially altered by heating up to 200°C.

As noted above, during diagenesis smectites commonly undergo an irreversible transition to illite through an interstratified illite/smectite intermediate. The extent of this reaction in pelitic sediments can be used as an approximate geothermometer (Hoffman et al. 1979), and it is thus essential to examine the extent of this reaction in the tuffs at the Nevada Test Site. The degree of interstratification in the montmorillonite-beidellites was examined using the techniques of Reynolds et al. (1970) and Srodon (1980). Table III lists the results of these determinations, along with the approximate ethylene-glycol-complex layer thickness. The montmorillonite-beidellites are all randomly interstratified with a small proportion of illite, and no ordered interstratifications are present. In all samples with low clay mineral contents, I estimated the degree of interstratification using the relative intensity of the low-angle scattering. However, this technique is beset by numerous problems connected with crystallite size and instrumental factors (Reynolds 1968; Ross 1968), and these results are only qualitative. I applied Srodon's (1980) methods to samples with more than 5% smectite, and these results are considerably more accurate; the uncertainties applied in Table III for these smectites are conservative. It is obvious from these results that there is no consistent trend in the degree of interstratification with depth, and the amount of illite is fairly uniform throughout the Bullfrog and Tram

TABLE III

X-RAY DIFFRACTION RESULTS FOR RANDOMLY INTERSTRATIFIED
ILLITE/SMECTITES IN USW-G1

Sample Number	Depth (m)	Per cent Illite in Illite/Smectite	Ethylene Glycol Complex Thickness (Å)
G1-2198	670.0	20±10	16.90
G1-2318	706.5	20±10	16.80
G1-2349	716.0	25±10	16.70
G1-2436	742.5	20±10	16.75 ^b
G1-2467	751.9	20±20 ^a	n.d. ^b
G1-2486	757.7	20±20 ^a	n.d.
G1-2525	769.6	25±20 ^a	16.70
G1-2613	796.4	30±20 ^a	16.75
G1-2622	799.2	30±20 ^a	n.d.
G1-2641	805.0	30±10	16.80
G1-2715	827.5	30±20 ^a	n.d.
G1-2748	837.6	10±10	16.80
G1-2804	854.7	30±20 ^a	n.d.
G1-2820	859.5	10±10	16.70
G1-2868	874.2	30±20 ^a	n.d.
G1-2884	879.0	30±20 ^a	n.d.
G1-2932	893.9	30±20 ^a	n.d.
G1-2981	908.6	30±20 ^a	n.d.
G1-3001	914.7	10±10	16.70
G1-3039	926.3	30±20 ^a	n.d.
G1-3099	944.6	5±5	16.75
G1-3137	956.2	15±10	16.75
G1-3196	974.1	20±10	16.75
G1-3238	986.9	10±10	16.85
G1-3258	993.0	25±10	16.90
G1-3321	1012.2	10±10	16.90
G1-3345	1019.6	5±5	16.90
G1-3371	1027.5	15±10	16.90
G1-3468	1057.0	5±5	16.85
G1-3500	1066.8	5±5	16.90

^a Estimated from low-angle scattering.

^b n.d. not determined.

Members, averaging about $10 \pm 10\%$. There is some variation in the thickness of the ethylene glycol complex reflecting changes in the layer charges of the montmorillonite-beidellites.

In the tuffs, the diagenetic transformation from smectite to illite has proceeded only slightly, if at all, and this is contrary to expectations based on the maximum paleogeotherm (Bish et al. 1981) and observations in pelitic sediments. Bish et al. reported that zeolite zone boundaries suggested temperatures between 75°C at the top of the Bullfrog Member and 110°C at the bottom of the Tram Member. The temperature currently ranges from 35-45°C. It thus appears that either (a) the reaction kinetics in the tuffs are significantly slower than in typical pelitic sediments, or (b) the smectites in the tuffs result from later alteration at temperatures more closely approaching

the current geotherm than the maximum paleogeotherm. Roberson et al. (1981) have shown that the reaction of smectite to interstratified illite/smectite is significantly inhibited by sodium, calcium, and magnesium in solution in addition to potassium. Indeed, Wolfsberg et al. (1979) report considerably more calcium (13 meq/l) and sodium (50 meq/l) than potassium (4.7 meq/l) in the water from J-13 well. It is therefore probable that the solution chemistry in the tuffs has a pronounced effect on the rate of the smectite to illite/smectite reaction. Considering the relatively steep paleogeotherm, it is equally likely that the smectites formed under conditions more closely approaching the present; Perry et al. (1970) showed that smectites are typically only 20% expandable by 100°C in Gulf Coast sediments. It appears certain that the zeolites and smectites formed under separate conditions and at different times in the tuffs at the Nevada Test Site.

VI. SUMMARY AND CONCLUSIONS

The results of a detailed examination of the mineralogy of the Bullfrog and Tram Members in USW-G1 agree closely with the bulk mineralogies determined by Bish et al. (1981), although I found slightly higher smectite contents in this study. Smectites are ubiquitous in both units, but a narrow range in the Bullfrog contains virtually no clay minerals. There are no apparent correlations between the amounts of smectite and the amounts of zeolite, quartz, and alkali feldspar, nor does the amount of smectite appear to be related to the degree of welding in the tuffs. In the Bullfrog, the zeolitized zones are poorest in smectite, and relatively abundant smectites and zeolites occur together in the lower Tram. The slightly welded to unwelded zone near the bottom of the Bullfrog contains very small amounts of smectites, suggesting that zeolitization may have lowered the initial high permeability. If so, this implies that smectite formation postdates zeolite crystallization in tuffs.

The montmorillonite-beidellites are randomly interstratified with typically $10 \pm 10\%$ illite, and there is no increase in degree of interstratification with depth. It is likely that the sodium, calcium-rich ground water inhibited the diagenetic smectite-to-illite transformation, but it is also probable that the smectites formed under conditions close to those in the rocks today (35-45°C) rather than under those suggested by the zeolite zone boundaries (75-110°C).

The smectites in the Bullfrog and Tram are all dominantly sodium-saturated montmorillonite-beidellites with typical layer charges and no high-charge layers. Sodium-saturated smectites exhibit a large variation in basal spacing (from 10 Å to 20 Å) with minor changes in temperature and humidity, and under room conditions, the basal spacings typically are 12.6 Å. Conditions in the saturated zone in situ are very likely considerably different, yielding smectites with basal spacings appreciably larger than 12.6 Å.

In view of the large possible variations in montmorillonite-beidellite volume and water content with small changes in temperature and relative humidity, it is imperative that we understand the present conditions (temperature and water pressure) in the tuffs and appreciate the changes in rock and mineral properties expected when altering these conditions, either in a repository or in a laboratory test. The effects of varying conditions on rock strength, porosity, and permeability should be carefully examined, and a detailed study of the effects of varying temperature and water pressure on the zeolites and clay minerals in the tuffs should be undertaken. Minor heating of the tuffs and concomitant collapse of the smectites could lead to the opening of fractures and release of free water, but the highly expandable sodium-smectites disseminated throughout the rocks could equally act as efficient barriers to fluid flow, immediately swelling in a hydrous atmosphere and effectively controlling permeability. Clearly, we should examine the expansion-collapse behavior of the montmorillonite-beidellites in environments closely approaching those in the tuffs, that is, heating in hydrous atmospheres rather than under room humidity conditions. It is also important to know the mode of occurrence of the smectites in tuffs and the minerals occurring in the pore spaces. The clays will have quite varying effects depending upon whether they occur in fractures, lining pores in the groundmass, or as massive alteration products of pumice fragments.

ACKNOWLEDGMENTS

I wish to thank J. Purson who prepared samples and K. Lombardo who prepared samples, performed clay mineral separations, and x-rayed numerous samples; their help allowed the clay mineral studies to proceed smoothly.

REFERENCES

- L. L. Ames, L. B. Sand, and S. S. Goldich, "A Contribution on the Hector, California, Bentonite Deposit," *Econ. Geol.* 53, 22-37 (1958).
- D. L. Bish, F. A. Caporuscio, J. F. Copp, B. M. Crowe, J. D. Purson, J. R. Smyth, and R. G. Warren, "Preliminary Stratigraphic and Petrologic Characterization of Core Samples from USW-G1, Yucca Mountain, Nevada," Los Alamos National Laboratory report LA-8840-MS (1981).
- J. R. Boles and S. G. Franks, "Clay Diagenesis in Wilcox Sandstones of Southwest Texas: Implications of Smectite Diagenesis on Sandstone Cementation," *Journ. Sed. Pet.* 49, 55-70 (1979).
- G. W. Brindley and G. Pedro, "Meeting of the Nomenclature Committee of A.I.P.E.A.," *Clays and Clay Min.* 23, 413-414 (1975).
- J. F. Burst, "Post Diagenetic Clay Mineral-Environmental Relationships in the Gulf Coast Eocene," *Clays and Clay Min.* 6, 327-341 (1959).
- P. I. Carroll, F. A. Caporuscio, and D. L. Bish, "Further Description of the Petrology of the Topopah Spring Member of the Paintbrush Tuff in Drill Holes UE25A-1 and USW-G1, and of the Lithic-Rich Tuff in USW-G1, Yucca Mountain, Nevada," Los Alamos National Laboratory report LA-9000-MS (1981).
- W. A. Deer, R. A. Howie, and J. Zussman, *An Introduction to the Rock-Forming Minerals*, (J. Wiley and Sons, Inc., New York, 1966), p. 266.
- B. R. Erdal, B. P. Bayhurst, B. M. Crowe, W. R. Daniels, D. C. Hoffman, F. O. Lawrence, J. R. Smyth, J. L. Thompson, and K. Wolfsberg, "Laboratory Studies of Radionuclide Transport in Geologic Media," *Underground Disposal of Radioactive Wastes*, Vol. II 367-382 (1980).
- F. H. Gillery, "Adsorption-Desorption Characteristics of Synthetic Montmorillonoids in Humid Atmospheres," *Am. Min.* 44, 806-818 (1959).
- R. Greene-Kelley, "Dehydration of the Montmorillonite Minerals," *Min. Mag.* 30, 604-615 (1955).
- R. E. Grim, *Clay Mineralogy* (McGraw-Hill Book Co., New York, 1953), p. 56.
- J. Hoffman and J. Hower, "Clay Mineral Assemblages as Low Grade Metamorphic Geothermometers: Application to the Thrust Faulted Disturbed Belt of Montana, U.S.A.," in *Aspects of Diagenesis*, P. A. Scholle and P. R. Schluger, eds., *Soc. Econ. Paleontol. Min. Spec. Public.* 26 (1979), pp. 55-80.
- J. Hower, "X-ray Diffraction Identification of Mixed-Layer Clay Minerals," in *Clays and The Resource Geologist*, F. J. Longstaffe, ed., *Min. Assoc. of Canada*, Toronto (1981), pp. 39-59.
- J. Hower, E. V. Eslinger, M. E. Hower, and E. A. Perry, "Mechanism of Burial Metamorphism of Argillaceous Sediments: I. Mineralogical and Chemical Evidence," *Bull. Geol. Soc. Am.* 87, 725-737 (1976).

F. J. Longstaffe, Clays and the Resource Geologist (Min. Assoc. of Canada) Short Course Notes 7 (1981).

D. M. C. MacEwan and A. Ruiz-Amil, "Interstratified Clay Minerals," in Soil Components, Inorganic Components, J. E. Gieseking, ed., Springer-Verlag, New York (1975), p. 271.

K. Norrish, "Forces Between Clay Particles," Intern. Clay Conf. Preprints Vol. 2, pp. 3-14 (1972).

W. C. Ormsby and L. B. Sand, "An Analytical Tool for Mixed-Layer Aggregates," Proc. Natl. Conf. Clays and Clay Min., Natl. Acad. Sci. Natl. Res. Council, 327, 254-263 (1954).

E. A. Perry and J. Hower, "Burial Diagenesis of Gulf Coast Pelitic Sediments," Clays and Clay Min. 18, 165-177 (1970).

E. A. Perry and J. Hower, "Late State Dehydration in Deeply Buried Pelitic Sediments," Bull. Am. Assoc. Petrol. Geolog. 56, 2013-2021 (1972).

R. C. Reynolds, Jr., "The Effect of Particle Size on Apparent Lattice Spacings," Acta Cryst. A24, 319-320 (1968).

R. C. Reynolds, Jr. and J. Hower, "The Nature of Interlayering in Mixed-Layer Illite-Montmorillonites," Clays and Clay Min. 18, 25-36 (1970).

H. E. Roberson and R. W. Lahann, "Smectite to Illite Conversion Rates: Effects of Solution Chemistry," Clays and Clay Min. 29, 129-135 (1981).

M. Ross, "X-ray Diffraction Effects by Nonideal Crystals of Biotite, Muscovite, Montmorillonite, Mixed-Layer Clays, Graphite, and Periclase," Zeit. für Krist. 126, 80-97 (1968).

J. R. Smyth, J. Thompson, and K. Wolfsberg, "Microautoradiographic Studies of the Sorption of U and Am on Natural Rock Samples," Rad. Waste Man. 1, 13-24 (1980).

R. W. Spengler, F. M. Byers, Jr., and J. B. Warner, "Stratigraphy and Structure of Volcanic Rocks in USW-G1, Yucca Mountain, Nye County, Nevada," U.S. Geol. Survey Open File Report, (in preparation).

R. W. Spengler, D. C. Muller, and R. B. Livermore, "Preliminary Report on the Geology and Geophysics of Drill Hole UE25a-1, Yucca Mountain, Nevada Test Site," U.S. Geol. Survey Open-File Report 79-1244, 43 p. (1979).

J. Srodon, "Precise Identification of Illite/Smectite Interstratifications by X-ray Powder Diffraction," Clays and Clay Min. 28, 401-411 (1980).

H. Suquet, C. De Le Calle, and H. Pezerat, "Swelling and Structural Organization of Saponite," Clays and Clay Min. 23, 1-9 (1975).

M. L. Sykes, G. H. Heiken, and J. R. Smyth, "Mineralogy and Petrology of Tuff Units from the UE25a-1 Drill Site, Yucca Mountain, Nevada," Los Alamos Scientific Laboratory report LA-8139-MS (1979).

C. E. Weaver and L. D. Pollard, The Chemistry of Clay Minerals (Elsevier Scientific Publishing Co., New York, 1975), p. 69.

K. Wolfsberg, B. P. Bayhurst, B. M. Crowe, W. R. Daniels, B. R. Erdal, F. O. Lawrence, A. E. Norris, and J. R. Smyth, "Sorptions-Desorption Studies on Tuff I. Initial Studies with Samples from the J-13 Drill Site, Jackass Flats, Nevada," Los Alamos Scientific Laboratory report LA-7480-MS (April 1979).